

# MAGIC ANGLE SPINNING CARBON-13 NMR OF TOBACCO MOSAIC VIRUS

## AN APPLICATION OF HIGH-RESOLUTION SOLID-STATE NMR SPECTROSCOPY TO VERY LARGE BIOLOGICAL SYSTEMS

M. A. HEMMINGA, W. S. VEEMAN, H. W. M. HILHORST, AND T. J. SCHAAFSMA,  
*Department of Molecular Physics, Agricultural University, 6700 EP Wageningen, The Netherlands, and Department of Physical Chemistry, University of Nijmegen, 6525 ED Nijmegen, The Netherlands*

**ABSTRACT** Magic angle spinning  $^{13}\text{C}$  NMR was used to study tobacco mosaic virus (TMV) in solution. Well-resolved  $^{13}\text{C}$  NMR spectra were obtained, in which several carbon resonances of amino acids of the TMV coat protein subunits that are not observable by conventional high-resolution NMR spectroscopy can be assigned. RNA resonances were absent, however, in the magic angle spinning  $^{13}\text{C}$  NMR spectra. Since three different binding sites are available for each nucleotide of the RNA, this is probably due to a line broadening caused by distributions of isotropic chemical shift values. In  $^{13}\text{C}$ -enriched TMV  $^{13}\text{C}$ - $^{13}\text{C}$  dipolar interactions also gave rise to line broadening. By suitable pulse techniques that discriminate carbon resonances on the basis of their  $T_1$  and  $T_{1\rho}$  values, it was possible to select particular groups of carbon nuclei with characteristic motional properties. Magic angle spinning  $^{13}\text{C}$  NMR spectra obtained with these pulse techniques are extremely well resolved.

### INTRODUCTION

Tobacco mosaic virus (TMV) is a well-known virus that infects tobacco plants. The molecular weight of the virus is  $42 \times 10^6$ , and the rod-like particle has a length of 300 nm and an outer diameter of 18 nm. The virus contains 2,200 identical protein subunits, each of molecular weight 17,500, which are helically complexed with a single strand of RNA 6,600 nucleotides long; each protein subunit binds three nucleotide bases (for a review, see Anderer, 1963; Caspar, 1963).

From structural (Stubbs et al., 1977; Bloomer et al., 1978) and biochemical (Butler and Klug, 1971; Zimmern and Butler, 1977; Jonard et al., 1977; Butler et al., 1977; Lebeurier et al., 1977) studies much is known about the three-dimensional structure of the virus and the protein-RNA interaction during the assembly of TMV (for a review, see Holmes, 1980). In principle, NMR can be used to obtain additional information about the structure and dynamics of the virus. In our laboratory, high-resolution NMR has been employed to study TMV and its protein (De Wit et al., 1978 and 1979). In 12%  $^{13}\text{C}$ -enriched TMV we found that some parts of the virus have a degree of internal mobility so high that  $^{13}\text{C}$  NMR resonances can be observed: 6% of the carbons of the backbone can be seen, and 17% of the aliphatic carbons appear in the spectrum (De Wit et al., 1979). Because the overall rotational motion of the virus in solution is very slow,  $^{13}\text{C}$  NMR resonances from the more rigid parts of

the virus are so strongly broadened by dipolar interactions and chemical shift anisotropy that they are not observable. Similar results have been obtained from  $^1\text{H}$  NMR experiments (De Wit et al., 1978; Jardetzky et al., 1978).

Although certain regions of the virus can be observed by conventional high-resolution NMR, it is impossible to obtain information about the rigid parts of the virus. Therefore, a logical step is to employ high-resolution NMR techniques for solids in studying TMV in solution.

In the last decade considerable progress has been made in the field of high-resolution NMR of solids. Line broadening due to dipolar interactions and chemical shift anisotropy can be largely eliminated. This is especially true for  $^{13}\text{C}$  NMR, where line broadening due to carbon-proton dipolar couplings is eliminated by proton decoupling and line broadening due to chemical shift anisotropy by magic angle spinning (for a review, see Schaefer and Stejskal, 1979). Cross-polarization of proton and carbon magnetization can be used for sensitivity enhancement (Pines et al., 1973).

In this paper we will demonstrate that high-resolution techniques for solids can be successfully applied to solutions of large biosystems, such as TMV. These line-narrowing techniques make it possible to observe  $^{13}\text{C}$  NMR resonances of the rigid parts in TMV. Some preliminary results have been published (Hemminga et al., 1981).

## EXPERIMENTAL METHODS

TMV strain *Vulgare* was prepared by polyethylene glycol precipitation followed by two differential centrifugation steps (Leberman, 1966). The preparation of  $^{13}\text{C}$ -enriched TMV is described elsewhere (De Wit et al., 1981). The average  $^{13}\text{C}$ -enrichment was determined to be  $\sim 12\%$  (De Wit et al., 1981). For the NMR experiments the virus was centrifuged for 1.5 h at 100,000  $g$  in a 10 mM phosphate buffer, pH 7.0. At 100% relative humidity the gellike virus pellet was transferred to a magic angle spinner. After filling, the spinner contained about 100 mg of virus. Concentration-dependent NMR experiments were carried out by diluting the virus pellet with the phosphate buffer. After the NMR experiments the integrity of the TMV was checked by electron microscopy.

The NMR experiments were performed at room temperature on a double-resonance spectrometer built around a wide-bore 4.2-T superconducting magnet Oxford Instruments Co. Ltd., England. Two  $\sim 150\text{-W}$  power amplifiers provided radio frequency fields at the proton (180 MHz) and carbon frequency (45 MHz) with rotating component amplitudes corresponding to a frequency of 35 kHz. Both proton-enhanced (Pines et al., 1973) and straightforward proton-decoupled  $^{13}\text{C}$  NMR were performed, also in combination with  $T_1$  or  $T_{1\rho}$  experiments (Veeman et al., 1979). The KEL-F magic angle spinner is cylindrical and is supported by two air bearings that are independent of the compressed air drive (Van Dijk et al., 1980). This spinner can be used for solid as well as for liquid samples. The magnet inhomogeneity over the sample in the spinner was  $\sim 2$  Hz.

## RESULTS AND DISCUSSION

Fig. 1 *A* shows a 45-MHz proton-enhanced and proton-decoupled magic angle spinning natural abundance  $^{13}\text{C}$  NMR spectrum of TMV in a gellike solution. The indicated resonances can be assigned, using the chemical shift data of James (1975). It is striking that this spectrum shows nearly as much detail and resolution as the spectrum obtained with conventional high-resolution  $^{13}\text{C}$  NMR on a 12%  $^{13}\text{C}$ -enriched sample of dissociated virus in which free protein subunits and RNA are present (see Fig. 1 *B*) (De Wit et al., 1979). In this sample, line-broadening effects from dipolar interactions and chemical shift anisotropy are eliminated by fast overall motion of the protein subunits. Also, local motions in the RNA are

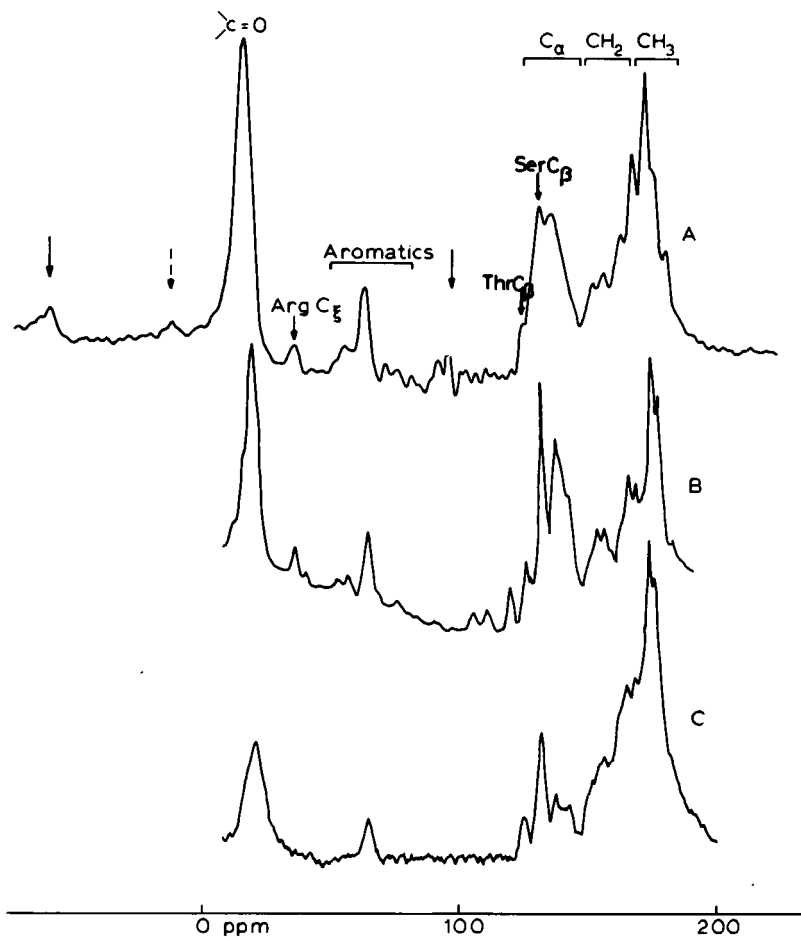


FIGURE 1 (A) 45-MHz proton-enhanced and proton-decoupled magic angle spinning natural abundance  $^{13}\text{C}$  NMR spectrum of 100 mg of TMV in 10 mM phosphate buffer, pH 7.0, at room temperature. Conditions: spinning rate, 3.4 kHz; cross-polarization time, 1 ms; 50,000 accumulations. The dotted arrow indicates a spinning side band of the main aromatic resonance; the solid arrows indicate side bands of the carbonyl resonance. (B) 90.5-MHz broad-band proton-decoupled  $^{13}\text{C}$  NMR spectrum of dissociated 12%  $^{13}\text{C}$ -enriched TMV with a concentration of 60 mg/ml (1 ml total volume) in 1 mM phosphate buffer, pH 11, at 30°C. Conditions: pulse repetition time, 1 s; sensitivity enhancement, 30 Hz; 50,000 accumulations. (C) 90.5-MHz broad-band proton-decoupled  $^{13}\text{C}$  NMR spectrum of native 12%  $^{13}\text{C}$ -enriched TMV in 1 mM phosphate buffer, pH 7.2. Other conditions: see B. Note that the vertical scales of B and C are different. The parts per million scale is referenced to  $\text{CS}_2$ , assuming 126 ppm for the Thr  $\text{C}_\alpha$  resonance.

then possible, as can be seen from the presence of RNA-sugar resonances in the region from 100 to 120 ppm. It has been shown that in this sample all carbons contribute to the  $^{13}\text{C}$  NMR spectrum (De Wit et al., 1979). For comparison, the conventional high-resolution  $^{13}\text{C}$  NMR spectrum of 12%  $^{13}\text{C}$ -enriched native TMV is given in Fig. 1 C.

The good resolution in the  $^{13}\text{C}$  NMR spectrum in Fig. 1 A indicates that there is no or only a small distribution of isotropic chemical shift values of equivalent carbons in the protein subunits in TMV. This is in agreement with structural studies of TMV, where a highly

symmetrical arrangement of the subunits is found (Caspar, 1963). By symmetry, all sites will then have the same isotropic chemical shift values. RNA-sugar resonances are observable in the region from 100 to 120 ppm in the  $^{13}\text{C}$  NMR spectrum in Fig. 1 *B* but are absent in the magic angle spinning  $^{13}\text{C}$  NMR spectrum in Fig. 1 *A*. It must be concluded that these resonances are broadened beyond detection, even under magic angle spinning. This can be the case if there is a broad distribution of isotropic chemical shift values of the RNA-sugar carbons. A distribution of isotropic chemical shifts is a common effect in high-resolution  $^{13}\text{C}$  NMR spectra of solid polymers (Schaefer and Stejskal, 1979) and amino acids.<sup>1</sup> Since three different binding sites are present for each nucleotide in TMV, this effect may arise from different environments for the RNA-sugar sites, possibly by differences in ring-current effects from adjacent aromatic rings of the protein subunits. Another, but less likely, possible explanation for the absence of RNA-sugar resonances, however, is a dipolar broadening due to  $^{31}\text{P}$  of the RNA-phosphate.

In Fig. 1 *A* magic angle sample spinning side bands of the carbonyl resonance can be observed. A similar side band of the main aromatic resonance is present as well. The side bands shift when the spinning frequency is changed. Such side bands, which appear when the spinning frequency is comparable to the chemical shift anisotropy (Schaefer and Stejskal, 1979), prove that most of the carbonyl and aromatic carbons are located in the rigid regions of the virus. No side bands of the aliphatic carbons appear in Fig. 1 *A*. This is clear, because the chemical shift anisotropy of aliphatic carbons ( $\sim 20$  ppm) is an order of magnitude smaller than the anisotropy of carbonyl and aromatic carbons ( $\sim 200$  ppm) (Pines et al., 1972). The arginine  $\text{C}_\gamma$  resonance is visible in Fig. 1 *A* but absent in the conventional high-resolution  $^{13}\text{C}$  NMR spectrum of native TMV (Fig. 1 *C*). Therefore, the arginines must also be located in the rigid parts of the protein subunits.

Taking into account all factors affecting the signal-to-noise ratio of the NMR spectra in Fig. 1 *A* and *B*, such as NMR frequency, sample volume and concentration, filling factors of probes, and the  $^{13}\text{C}$ -enrichment of TMV in Fig. 1 *B*, it can be concluded that the proton-enhanced magic angle spinning NMR technique has better sensitivity than the conventional high-resolution NMR method. This gain in sensitivity is due to cross-polarization of the proton and carbon magnetization and, especially, to the fact that with magic angle spinning all carbons of the virus contribute to the spectrum. With conventional NMR only the mobile carbons contribute to the spectrum.

It can be seen that the carbonyl resonance in Fig. 1 *A* is somewhat broader than the other resonances. This line width is not only due to an inhomogeneous broadening mechanism, i.e., a distribution of chemical shifts but may also be due to a homogeneous broadening arising from couplings to the  $^{14}\text{N}$  in the protein backbone. An example for such a homogeneous broadening of the carbonyl resonance has been found in magic angle spinning  $^{13}\text{C}$  NMR spectra of solid oligopeptides. In these systems, it is observed that carbon resonances can be broadened by the  $^{14}\text{N}$  quadrupole moment interfering with the ability of magic angle sample spinning to suppress the  $^{13}\text{C}$ - $^{14}\text{N}$  dipolar interaction.<sup>1,2</sup> Also, the resonance of the  $\alpha$ -carbons and arginine

<sup>1</sup>Opella, S. J., J. G. Hexem, M. H. Frey, and T. A. Cross. Solid state NMR of biopolymers. Submitted for publication.

<sup>2</sup>Hexem, J. G., M. H. Frey, and S. J. Opella. Influence of  $^{14}\text{N}$  on  $^{13}\text{C}$  NMR spectra of solids. Submitted for publication.

$C_T$  should be influenced by the  $^{13}\text{C}$ - $^{14}\text{N}$  interaction. A slight indication for this may be found by a comparison of these resonances in Fig. 1 *A* and *B*.

Proton-enhanced magic angle spinning  $^{13}\text{C}$  NMR spectra were also obtained from solutions of TMV with increasing water content by diluting the gellike virus pellet. Apart from a reduction of signal-to-noise ratio in the spectra, no effect of dilution on the spectral line shape could be observed. This indicates that in our experiments the virus concentration can be as high as possible. This favors rapid spectra accumulation, the virus still being in its natural aqueous environment (the water content of a TMV pellet is still  $\sim 70\%$ ). Electron micrographs of TMV samples were taken after the NMR experiments. No degradation of the virus by magic angle sample spinning was observed.

To speed up the experiments, magic angle spinning NMR measurements were carried out with  $^{13}\text{C}$ -enriched TMV. This was especially important for relaxation time measurements, which are very time consuming. The proton-enhanced magic angle spinning  $^{13}\text{C}$  NMR spectrum of 12%  $^{13}\text{C}$ -enriched TMV is shown in Fig. 2 *A*. Spectra with good signal-to-noise ratios result, but an unexpected line broadening occurs, which is especially noticeable for the aromatic resonances. This broadening may be caused by  $^{13}\text{C}$ - $^{13}\text{C}$  dipolar couplings in 12%  $^{13}\text{C}$ -enriched TMV. In the case of like spins, magic angle sample spinning is not able to completely remove dipolar couplings (Maricq and Waugh, 1979). Another possibility may be

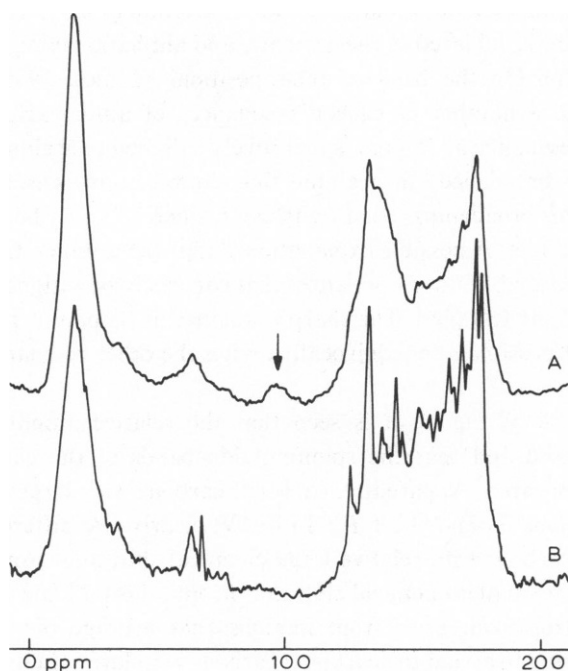


FIGURE 2 (A) 45-MHz proton-enhanced and proton-decoupled magic angle spinning  $^{13}\text{C}$  NMR spectrum of 12%  $^{13}\text{C}$ -enriched TMV. Conditions: see caption to Fig. 1 *A*. The arrow indicates a spinning side band of the carbonyl resonance. (B) 45-MHz magic angle spinning  $^{13}\text{C}$  NMR spectrum of 12%  $^{13}\text{C}$ -enriched TMV. Conditions: pulse repetition time, 0.25 s; spin-lock time, 1 ms. Other conditions: see caption to Fig. 1 *A*.

that random molecular motions on a relatively slow time scale produce a broadening by interfering with the averaging produced by magic angle spinning (Suwelack et al., 1980).

By  $^{13}\text{C}$  enrichment the probability of  $^{13}\text{C}$ - $^{13}\text{C}$  pairs increases, resulting in a broadening of the  $^{13}\text{C}$  NMR spectrum (Fig. 2*A* as compared to Fig. 1*A*). From simple statistical considerations and assuming a random  $^{13}\text{C}$  distribution in the virus, it would be expected that the probability of  $^{13}\text{C}$ - $^{13}\text{C}$  pairs in aromatic rings is larger than the probability in other amino acid side chains, which would result in strongly broadened aromatic resonances. Nonrandom isotope distributions, which have been shown to exist (De Wit et al., 1981) will even increase the probability of  $^{13}\text{C}$ - $^{13}\text{C}$  pairs.

Nevertheless, the  $^{13}\text{C}$  NMR spectrum in Fig. 2*A* contains some resolved resonances, making it possible to carry out  $T_1$  and  $T_{1\rho}$  experiments. It was found that across the total spectrum there is not much difference between the shortest and longest values of  $T_1$  and  $T_{1\rho}$ . The values of  $T_1$  are estimated to be between  $\sim 0.25$  and 2 s; the  $T_{1\rho}$  values range from  $\sim 0.1$  to 1 ms. From these measurements it also follows that the relative broad resonances in the spectrum in Fig. 2*A* have relatively long values of  $T_1$  and short values of  $T_{1\rho}$ . This enables us to enhance the resolution of the  $^{13}\text{C}$  NMR spectrum by eliminating the relatively broad components.

Fig. 2*B* shows a  $^{13}\text{C}$  NMR spectrum of TMV obtained without proton enhancement but by straightforward  $^{13}\text{C}$   $90^\circ$  pulses applied every 0.25 s, immediately followed by a 1-ms  $^{13}\text{C}$  spin-lock pulse. In this way, carbons with a long  $T_1$  and short  $T_{1\rho}$  do not contribute to the spectrum. From a comparison of *A* and *B* of Fig. 2, it follows that in this way a remarkable resolution enhancement is achieved in the aromatic and aliphatic region, at the cost, however, of signal-to-noise ratio. On the basis of their positions (James, 1975) in the  $^{13}\text{C}$  NMR spectrum in Fig. 2*B*, a number of carbon resonances of amino acid side chains can be assigned. The small resonance at 35 ppm is tentatively assigned to arginine  $C_\gamma$ . In Fig. 2*A* this resonance is strongly broadened. In arginine this carbon atom is isolated from the other carbons. Therefore, this broadening is not quite clear, since it cannot be explained directly by a dipolar broadening effect. A possible explanation is that the arginine  $C_\gamma$  carbons are close to carbons of other amino acids. Other resonances that can easily be assigned are threonine  $C_\beta$  at 126 ppm and serine  $C_\beta$  at 133 ppm. The sharp resonance at 68 ppm is probably an impurity. At this stage, it is not possible to unequivocally assign the other resonances in the  $^{13}\text{C}$  NMR spectrum in Fig. 2*B*.

Comparing *A* and *B* of Fig. 2, it is seen that the relative amplitude of the carbonyl resonance has decreased and that the spinning side bands of the carbonyl and aromatic resonances have disappeared. Apparently, carbonyl carbons with large chemical shift anisotropy have a relative long  $T_1$  and short  $T_{1\rho}$ . In TMV, clearly two different kinds of carbonyl carbons are present: carbons with relative large chemical shift anisotropy, long  $T_1$  and short  $T_{1\rho}$ , and carbons with a smaller chemical shift anisotropy, short  $T_1$  and long  $T_{1\rho}$ . The smaller chemical shift anisotropy can arise from motions that average out at least part of the anisotropy. It is tempting to assign the carbonyl carbons with large chemical shift anisotropies to sites in the more rigid parts of the virus and the carbonyl carbons with smaller chemical shift to the more flexible regions of TMV. From these considerations, it is concluded that the whole  $^{13}\text{C}$  NMR spectrum in Fig. 2*B* arises from carbons in the mobile parts of TMV, parts, however, that are not as mobile as the carbons responsible for the conventional high-resolution

$^{13}\text{C}$  NMR spectrum in Fig. 1 C. In addition, in the spectrum in Fig. 2 B, no indication is found for line broadening by  $^{13}\text{C}$ - $^{13}\text{C}$  dipolar interactions, suggesting that these interactions are averaged out in the mobile virus parts. This experiment shows that using suitable pulse techniques it is possible to study groups of carbon nuclei with particular motion characteristics.

## CONCLUSIONS

It can be concluded from our NMR experiments that magic angle spinning  $^{13}\text{C}$  NMR with or without proton enhancement is a valuable technique for the study of high-molecular-weight biological systems with regular structures, such as TMV. Well-resolved  $^{13}\text{C}$  NMR spectra can be obtained, in which several carbon resonances of amino acids that are not observable in conventional high-resolution NMR spectroscopy can be assigned. In high-resolution solid state  $^{13}\text{C}$  NMR spectra, however, unusual line-broadening effects appear, such as those due to  $^{13}\text{C}$ - $^{14}\text{N}$  and  $^{13}\text{C}$ - $^{13}\text{C}$  dipolar interactions and distribution of isotropic chemical shift values, decreasing the spectral resolution. By suitable pulse techniques, it is possible to select particular groups of carbon nuclei with characteristic motion properties.

We are indebted to Dr. S. J. Opella for making available his results before publication.

Received for publication 29 January 1981 and in revised form 5 March 1981.

## REFERENCES

- Anderer, F. 1963. Recent studies on the structure of tobacco mosaic virus. *Adv. Protein Chem.* 18:1-35.
- Bloomer, A. C., J. N. Champness, G. Bricogne, R. Staden, and A. Klug. 1978. Protein disk of tobacco mosaic virus at 2.8 Å resolution showing the interactions within and between subunits. *Nature (Lond.)*. 276:362-368.
- Butler, P. J. G., J. T. Finch, and D. Zimmern. 1977. Configuration of tobacco mosaic virus RNA during virus assembly. *Nature (Lond.)*. 265:217-219.
- Butler, P. J. G., and A. Klug. 1971. Assembly of the particle of tobacco mosaic virus from RNA and disks of protein. *Nat. New Biol.* 229:47-50.
- Caspar, D. L. D. 1963. Assembly and stability of the tobacco mosaic virus particle. *Adv. Protein Chem.* 18:37-121.
- De Wit, J. L., N. C. M. Alma, and T. J. Schaafsma. 1980.  $^{13}\text{C}$  enrichment of tobacco mosaic virus. *Biochem. Biophys. Res. Commun.* 97:1053-1059.
- De Wit, J. L., N. C. M. Alma-Zeestraten, M. A. Hemminga, and T. J. Schaafsma. 1979. Carbon-13 nuclear magnetic resonance studies on tobacco mosaic virus and its protein. *Biochemistry*. 18:3973-3976.
- De Wit, J. L., M. A. Hemminga, and T. J. Schaafsma. 1978. A  $^{13}\text{C}$  and  $^1\text{H}$  NMR study of the dynamic behavior of tobacco mosaic virus protein. *J. Magn. Resonance*. 31:97-107.
- Hemminga, M. A., W. S. Veeman, H. W. M. Hilhorst, and T. J. Schaafsma. 1981. Magic angle spinning NMR of tobacco mosaic virus. *Bull. Magn. Resonance*. 2:344.
- Holmes, K. C. 1980. Protein-RNA interactions during the assembly of tobacco mosaic virus. *Trends Biochem. Sci.* 5:4-7.
- James, T. L. 1975. Nuclear magnetic resonance in biochemistry. Principles and applications. Academic Press, Inc., New York. 246-247.
- Jardetzky, O., K. Akasaka, D. Vogel, S. Morris, and K. C. Holmes. 1978. Unusual segmental flexibility in a region of tobacco mosaic virus coat protein. *Nature (Lond.)*. 273:564-566.
- Jonard, G., K. E. Richards, H. Guilley, and L. Hirth. 1977. Sequence from the assembly nucleation region of TMV RNA. *Cell*. 11:483-493.
- Leberman, R. 1966. The isolation of plant viruses by means of 'simple' coacervates. *Virology*. 30:341-347.
- Lebeurier, G., A. Nicolaieff, and K. E. Richards. 1977. Inside-out model for self-assembly of tobacco mosaic virus. *Proc. Natl. Acad. Sci. U.S.A.* 74:149-153.
- Maricq, M. M., and J. S. Waugh. 1979. NMR in rotating solids. *J. Chem. Phys.* 70:3300-3316.

- Pines, A., M. G. Gibby, and J. S. Waugh. 1972. Proton-enhanced nuclear induction spectroscopy.  $^{13}\text{C}$  chemical shielding anisotropy in some organic solids. *Chem. Phys. Lett.* 15:373-376.
- Pines, A., M. G. Gibby, and J. S. Waugh. 1973. Proton-enhanced NMR of dilute spins in solids. *J. Chem. Phys.* 59:569-590.
- Schaefer, J., and E. O. Stejskal. 1979. High-resolution  $^{13}\text{C}$  NMR of solid polymers. In *Topics in Carbon-13 NMR Spectroscopy*. G. C. Levy, editor. John Wiley & Sons, Inc., New York. 283-324.
- Stubbs, G., S. Warren, and K. C. Holmes. 1977. Structure of RNA and RNA binding site in tobacco mosaic virus from 4-Å map calculated from X-ray fibre diagrams. *Nature (Lond.)*. 267:216-221.
- Suwelack, D., W. P. Rothwell, and J. S. Waugh. 1980. Slow molecular motion detected in the NMR spectra of rotating solids. *J. Chem. Phys.* 73:2559-2569.
- Van Dijk, P. A. S., W. Schut, J. W. M. van Os, E. M. Menger, and W. S. Veeman. 1980. A high speed spinner for magic angle spinning NMR. *J. Phys. E Sci. Instrum.* 13:1309-1310.
- Veeman, W. S., E. M. Menger, W. Ritchey, and E. de Boer. 1979. High-resolution carbon-13 nuclear magnetic resonance of solid poly(oxyethylene). *Macromolecules*. 12:924-927.
- Zimmern, D., and P. J. G. Butler. 1977. The isolation of tobacco mosaic virus RNA fragments containing the origin for viral assembly. *Cell*. 11:455-462.